

Changes in perfusion and fatty acid metabolism of rat heart with autoimmune myocarditis

Eiichiro TSUJIMURA,* Hideo KUSUOKA,*# Kazuki FUKUCHI,* Shinji HASEGAWA,* Kenji YUTANI,* Masatsugu HORI,** Satoru HIRONO,*** Tohru IZUMI**** and Tsunehiko NISHIMURA*##

*Division of Tracer Kinetics, Biomedical Research Center, and **First Department of Medicine, Osaka University Medical School

***First Department of Medicine, Niigata University School of Medicine

****Department of Medicine, Kitasato University School of Medicine

#Osaka National Hospital and ##Kyoto Prefectural University of Medicine

To elucidate the change in perfusion and aerobic metabolism in myocarditis, tissue counting and dual tracer *ex vivo* autoradiography with Tl-201 and a free fatty acid analog, I-123- or I-125-labeled (p-iodophenyl)-methyl-pentadecanoic acid (BMIPP), were performed in rats with myocarditis induced by immunization with cardiac myosin. Inflammatory damage was classified histologically. At the acute stage (2–4 weeks after the antigen-injection), total heart uptakes of Tl and BMIPP and the ratio (BMIPP/Tl) were significantly reduced in myocarditis rats (N = 15) compared with the controls (N = 12). Myocardial distribution of Tl and BMIPP was not homogeneous. Relative uptake of Tl and BMIPP (N = 9, 128 regions) was gradually decreased with the extent of inflammation, and the regional BMIPP/Tl was smaller than the control. At the subacute stage (7 weeks after the antigen-injection), total Tl uptake in myocarditis rats (N = 5) recovered to the control level (N = 4), but that of BMIPP was still significantly lower than the control. BMIPP/Tl was still significantly lower in myocarditis. Myocardial distribution of Tl and BMIPP recovered to be more homogeneous. Relative uptake of Tl and BMIPP (N = 6, 78 regions) still gradually but significantly decreased with the extent of inflammation. Regional BMIPP/Tl was still depressed in myocarditis. These results indicate that myocardial perfusion and aerobic metabolism were discrepant and heterogeneously suppressed with severe inflammation during the acute stages, but the difference decreases with time. Examination with Tl-201 and BMIPP may provide information about the severity of myocarditis.

Key words: myocarditis, BMIPP, Tl-201, inflammation

INTRODUCTION

MYOCARDITIS sometimes causes sudden unexpected death or severe congestive heart failure.¹ Furthermore, it may contribute to the pathogenesis of idiopathic congestive cardiomyopathy,² but accurate detection of myocarditis is frequently difficult.³ The myocardial energy supply mainly depends on aerobic metabolism of free fatty acids (FFA).^{4,5}

Necrosis and fibrosis, or microcirculation disorder induced by inflammation would decrease tissue uptake of FFA, whereas increased energy demand might enhance the FFA uptake, so that, if myocarditis induces specific changes in perfusion and FFA metabolism, the detection of such changes may help in the diagnosis of myocarditis. But, little is known about these changes.

Several fatty acid analogs labeled with radionuclides such as C-11 and I-123 have recently been developed for the noninvasive evaluation of regional fatty acid metabolism.^{6–9} Radioiodinated 15-(p-iodophenyl)-3-R,S-methylpentadecanoic acid (BMIPP) is one of such analogs,¹⁰ and has been widely used for clinical imaging of myocardial fatty acid metabolism.¹¹

Received May 10, 2000, revision accepted August 10, 2000.

For reprint contact: Tsunehiko Nishimura, M.D., Ph.D., Division of Tracer Kinetics, Biomedical Research Center, Osaka University Medical School, 2–2 Yamada-oka, Suita, Osaka 565–0871, JAPAN.

This study focused on the changes in myocardial perfusion and free fatty acid metabolism induced by myocarditis at the acute and subacute stages. Dual tracer *ex vivo* autoradiography with ^{201}Tl and radioiodinated BMIPP was performed in rats with autoimmune myocarditis.

MATERIALS AND METHODS

Experimental myocarditis in rats was generated by immunization with cardiac myosin as described previously.¹² Briefly, cardiac myosin purified from the ventricular muscle of pig hearts by the standard method¹² was prepared and used as an antigen. The antigen was dissolved at a concentration of 20 mg/mL in phosphate-buffered saline (PBS) containing 0.3 mol/L KCl and mixed with an equal volume of complete Freund's adjuvant (CFA) containing 11 mg/mL of *Mycobacterium tuberculosis* (Difco Laboratories, Detroit MN). Antigen-adjuvant emulsion (0.2 mL) was injected subcutaneously into the footpads of male Lewis rats (8-weeks old). Another group of age-matched rats (control group, N = 16) received 0.1 mL of saline mixed with an equal volume of CFA. The rats were purchased from Charles River Japan Inc. (Hino, Japan) and maintained under specific pathogen-free conditions at the Facilities for Comparative Medicine and Animal Experimentation, Osaka University Medical School. All experiments followed the "Principles of laboratory animal care" (NIH publication No. 86-23, revised 1985), and the protocols were approved by the Committee of Animal Experiments of Osaka University Medical School.

Measurement of myocardial uptake of ^{201}Tl and ^{123}I -BMIPP

At 2–4 weeks after the antigen-injection (acute stage, N = 15)¹² or 7 weeks after the antigen-injection (subacute stage, N = 5),¹² the rats were anesthetized with pentobarbital (0.01 g/100 g body weight). ^{123}I -BMIPP (Nihon Mediphsics, Nishinomiya, Japan; 7.4 MBq) was injected from the tail vein, and 5 min later ^{201}Tl (7.4 MBq) was injected. The rats were sacrificed by injection of saturated KCl 30 min after the injection of ^{201}Tl . The heart was excised, blotted on filter paper, and weighed. The activity of ^{123}I -BMIPP and ^{201}Tl was measured in a single channel analyzer with a 2 × 2 NaI scintillator (Ohya Koken Kogyo, Tokyo, Japan). The myocardial uptake (% of injected dose; %ID) of ^{201}Tl and ^{123}I -BMIPP was calculated as follows¹⁴;

$$\begin{aligned} \text{myocardial uptake (\%)} \\ = \frac{\text{myocardial count / heart weight}}{\text{total injected dose / body weight}} \times 100 \end{aligned}$$

The rats injected only with adjuvant (CFA) served as the control for total myocardial uptake of Tl and BMIPP (N = 12 for the acute stage, N = 4 for the subacute stage).

Dual tracer autoradiography

Dual tracer autoradiography with ^{201}Tl and ^{125}I -BMIPP was performed at the acute (N = 9) and subacute (N = 6) stages of myocarditis or the control (N = 5 as indicated above). The protocol was similar to the previous one; rats were first injected intravenously with 1.85 MBq of ^{125}I -BMIPP, and later with 18.5 MBq of ^{201}Tl , then killed with KCl. The heart was rapidly excised, rinsed with saline, and cut at the midline of the left ventricle. The apical half of the heart was rapidly frozen in powdered dry ice and cut into 20- μm thick sections with a cryostat in the direction perpendicular to the longitudinal axis of the ventricle. The sections at the mid-ventricle were placed on glass cover slips, and on an imaging plate. The first autoradiographic exposure was performed for 1 hour to detect the distribution of ^{201}Tl . After a 30-day waiting period for ^{201}Tl decay, the second exposure was conducted for 10 days to obtain an adequate ^{125}I -BMIPP imaging. The injection doses were determined to minimize the effect of BMIPP on the first autoradiograph of Tl based on the preliminary experiments.

The image data were analyzed with a computerized imaging analysis system (Fuji Bio-Imaging Analyzer BAS 2000, Fuji Photo Film, Tokyo, Japan). To quantitate the regional uptake of ^{201}Tl or ^{125}I -BMIPP, ROI's (0.36 mm²) were set on each autoradiogram. The myocardial uptake of the ROI in the regions with normal histological features was used as the individual reference for each heart. The regional uptake at each ROI was normalized by this standard value. The rats injected only with adjuvant (CFA) also served as controls for regional uptake (N = 3 for the acute stage, N = 2 for the subacute stage). The hearts used for the measurement of total heart uptake and those for the regional uptake were completely separate in these experiments.

Histopathological assessment

The consecutive myocardial tissue used for autoradiography was also sectioned at a thickness of 10 μm , and stained with hematoxylin and eosin. The extent of inflammatory cell infiltration and that of myocyte necrosis were evaluated by two independent observers, and classified as follows: slight, lesions involving < 30% of the myocardium; moderate, lesions involving = 30% to 70% of the myocardium; and severe, lesions involving > 70% of the myocardium (Fig. 1).

Statistical analysis

Data are expressed as the mean \pm SE. Comparison among groups in each stage was done by one-way analysis of variance (ANOVA) with a multiple comparison test. Comparison within the group was done by paired Student's t-test. Probability less than 0.05 was considered to indicate a significant difference.

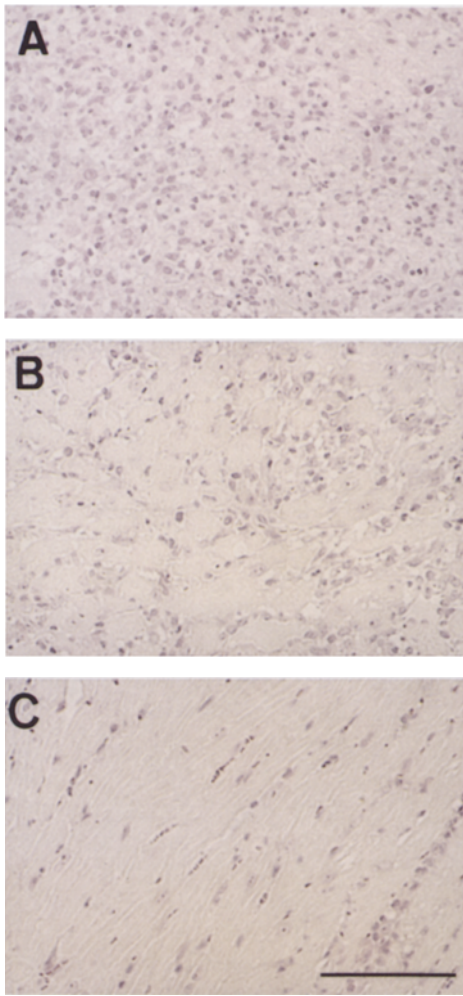


Fig. 1

Fig. 1 Pathological grading of the extent of inflammatory damage.

A: severe change, B: moderate change, C: slight change. The bar in the panel indicates 25 μm in length. (magnification $\times 200$)

Fig. 2 Body weight (A), heart weight (B), and heart weight-to-body weight ratio (C) at the acute and subacute stages of myocarditis.

Open and closed bars indicate control and myocarditis rats, respectively.

***: $p < 0.001$ vs. control.

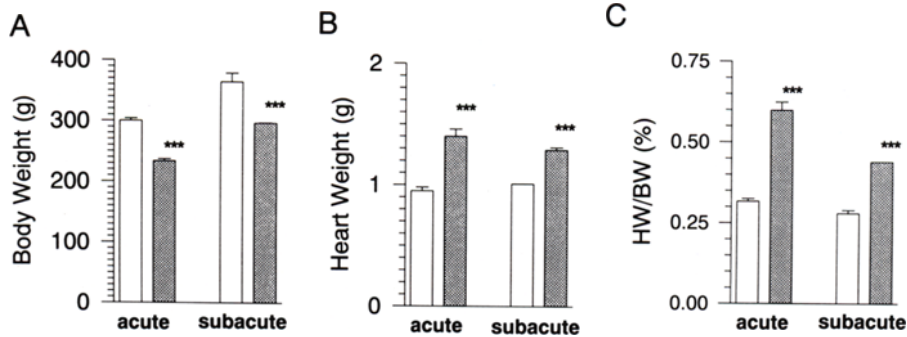


Fig. 2

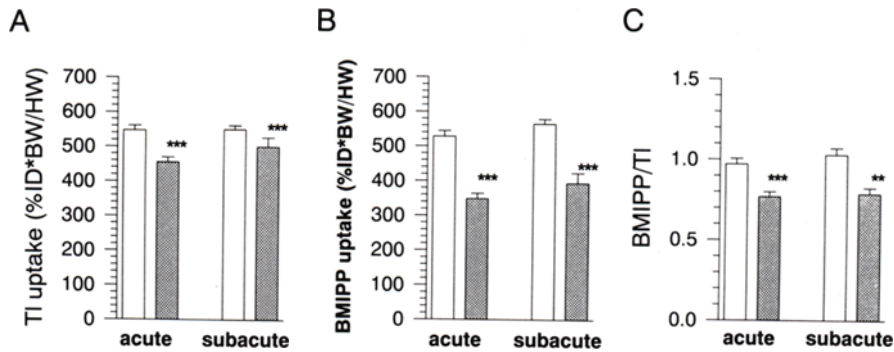


Fig. 3

Fig. 3 Total heart uptake of ^{201}Tl (A) and ^{123}I -BMIPP (B), and the ratio of ^{123}I -BMIPP uptake to ^{201}Tl one (C) at the acute and subacute stages.

Open and closed bars indicate control and myocarditis rats, respectively.

** , ***: $p < 0.01$ and $p < 0.001$ vs. control.

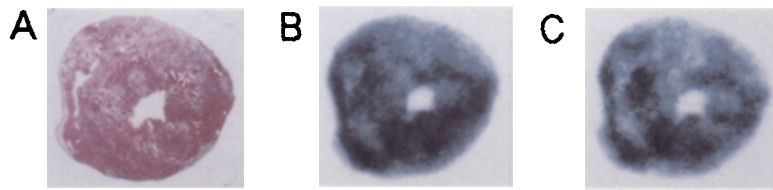


Fig. 4 Microscopic findings and dual-tracer autoradiograms at the acute stage. A: Hematoxylin and eosin staining (magnification $\times 2$). B: ^{201}Tl image. C: ^{125}I -BMIPP image.

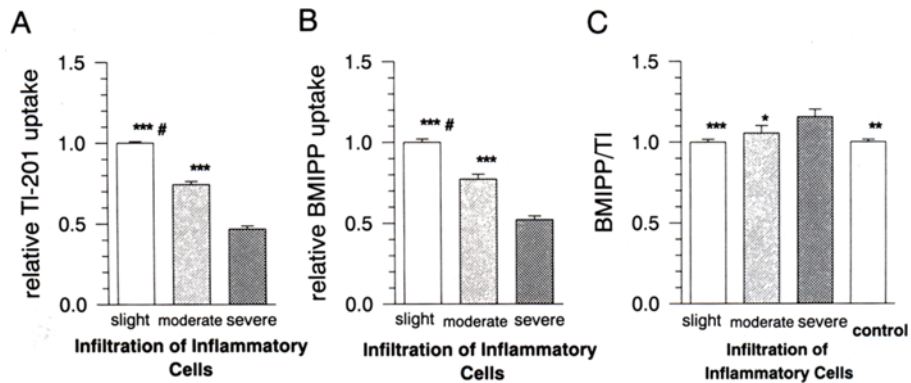


Fig. 5 Relative regional uptake of ^{201}Tl (A) and ^{125}I -BMIPP (B), and the relative regional uptake ratio of ^{125}I -BMIPP to ^{201}Tl (C) at different pathological grades of the inflammation at the acute stage. *, **, ***: $p < 0.05$, $p < 0.01$, and $p < 0.001$ vs. severe. #: $p < 0.001$ vs. moderate.

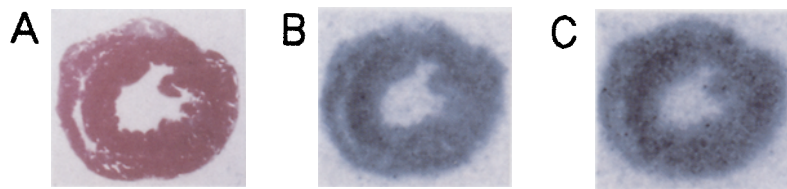


Fig. 6 Microscopic findings and dual-tracer autoradiograms at the subacute stage. A: Hematoxylin and eosin staining (magnification $\times 2$). B: ^{201}Tl image. C: ^{125}I -BMIPP image.

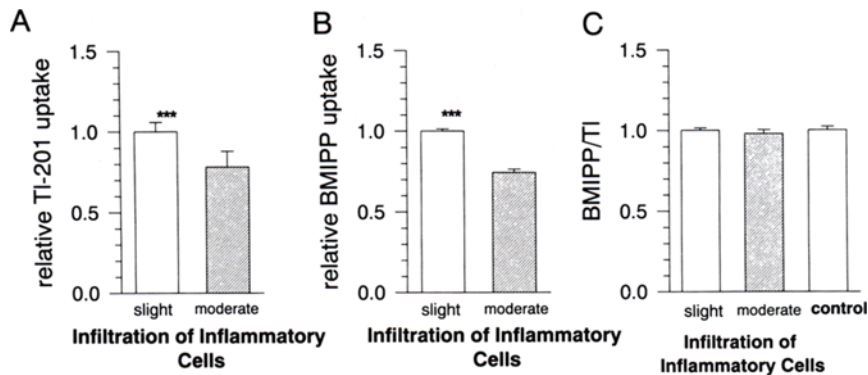


Fig. 7 Relative regional uptake of ^{201}Tl (A) and ^{125}I -BMIPP (B), and the relative regional uptake ratio of ^{125}I -BMIPP to ^{201}Tl (C) at different pathological grades of inflammation at the subacute stage. ***: $p < 0.001$ vs. moderate.

RESULTS

Changes in the whole heart

The measurement of body and heart weights was done in rats used for the measurement of total heart uptake. Both in the acute ($N = 15$) and subacute ($N = 5$) stages, rats with

myocarditis had significantly lighter body weight (Fig. 2A; $p < 0.001$) but heavier heart weight (Fig. 2B; $p < 0.001$) than the control rats ($N = 12$ for acute stage, $N = 4$ for subacute stage). The ratio of heart weight to body weight was therefore significantly greater in myocarditic rats than in controls (Fig. 2C; $p < 0.001$), indicating

myocardial hypertrophy. Furthermore, myocarditic rats showed signs of congestive heart failure such as subcutaneous edema, ascites, hydrothorax and hydropericardium. These results suggest that the cardiac function of the myocarditic rats was decompensated at both stages.

Total heart uptake at the acute stage of myocarditis (N = 15) was significantly reduced with both ^{201}Tl (Fig. 3A; $p < 0.001$) and ^{125}I -BMIPP (Fig. 3B; $p < 0.001$) compared with control rats (N = 12). At the subacute stage, total heart uptake of ^{201}Tl in myocarditic rats (N = 5) recovered to the level of control rats (N = 4; Fig. 3A), but that of ^{125}I -BMIPP was still significantly lower than controls (Fig. 3B; $p < 0.001$). The ratio of BMIPP to ^{201}Tl uptake was significantly lower in myocarditic rats both at the acute (Fig. 3C; $p < 0.001$) and subacute (Fig. 3C; $p < 0.01$) stages.

Regional changes at the acute stage

At the acute stage of myocarditis, scattered inflammatory foci of various sizes were observed, and some of them spread transmurally. The inflammatory lesions corresponded well with macroscopically discolored areas (Fig. 4A), in which microscopical findings were consistent with a previous report.¹²

Myocardial distribution of ^{201}Tl and ^{125}I -BMIPP was heterogeneous as shown in Figure 4. A region showing little histological damage was selected in each slice, and served as the control region. The myocardial uptake in each ROI was normalized by that in the control region, because no external standard was used. Relative ^{201}Tl uptake at regions with slight, moderate and severe inflammatory changes (Fig. 5A) were $100.0 \pm 0.9\%$ (44 regions selected from 9 hearts, $p < 0.001$ vs. moderate and severe), $74.3 \pm 1.9\%$ (38 regions, $p < 0.001$ vs. severe), and $46.7 \pm 1.9\%$ (46 regions), respectively. BMIPP autoradiograms were matched to corresponding ^{201}Tl autoradiograms. BMIPP uptake at regions with slight, moderate, and severe damage (Fig. 5B) were $100.0 \pm 2.1\%$ ($p < 0.001$ vs. moderate and severe), $77.3 \pm 3.0\%$ ($p < 0.001$ vs. severe), and $52.3 \pm 2.3\%$, respectively. Relative uptake of ^{201}Tl and BMIPP was significantly decreased with the extent of inflammation ($p < 0.001$). The ratio of BMIPP uptake to that of ^{201}Tl in the same region was increased to the same extent as inflammation (Fig. 5C). The ratio at the regions with severe damage (1.16 ± 0.47) was significantly higher than in any other region (slight, 1.00 ± 0.18 , $p < 0.001$; moderate, 1.06 ± 0.47 , $p < 0.05$). Similar analysis was done in the control rats (1.00 ± 0.01 , $p < 0.01$; 45 regions), but when this ratio was corrected by the ratio in a whole heart (0.77 ; Fig. 3C), the ratio ($1.16 \times 0.77 = 0.89$) was still smaller than the control ($1.00 \times 0.97 = 0.97$), indicating that regional BMIPP uptake is more depressed than that of ^{201}Tl at the acute stage.

Regional changes at the subacute stage

At the subacute stage, interstitial cellular infiltration and

edema had almost disappeared and been replaced by fibrosis (Fig. 6A). Inflammatory foci were rarely detected. There were few regions showing severe inflammatory changes. Myocardial distribution of ^{201}Tl and ^{125}I -BMIPP recovered to become more homogeneous than at the acute stage (Fig. 6B, C). Few regions showed any sign of severe inflammatory changes. Relative ^{201}Tl uptake in the regions with slight and moderate inflammatory changes (Fig. 7A) were $100.0 \pm 0.9\%$ (40 regions from 6 hearts, $p < 0.001$ vs. moderate), and $76.3 \pm 1.6\%$ (38 regions), respectively. BMIPP uptake in the regions with slight and moderate damage (Fig. 7B) were $100.0 \pm 1.4\%$ ($p < 0.001$ vs. moderate) and $74.5 \pm 1.9\%$, respectively. Relative regional uptake of ^{201}Tl and BMIPP was also gradually but significantly decreased with the extent of inflammation ($p < 0.001$). The regional ratios of BMIPP uptake to that of ^{201}Tl in the areas with slight change (1.00 ± 0.14) and moderate change (0.98 ± 0.15) were almost identical to those in control hearts (1.01 ± 0.01 , 17 regions; Fig. 7C). Correction by the ratio in a whole heart ($1.00 \times 0.79 = 0.79$ at slight change, $1.01 \times 1.03 = 1.04$ in control) indicated that regional BMIPP uptake was still more depressed than that of ^{201}Tl .

DISCUSSION

In this study, myocardial perfusion and free fatty acid metabolism in hearts with myocarditis were investigated by dual tracer *ex vivo* autoradiography with ^{201}Tl and radiolabeled BMIPP. Our results showed that perfusion and metabolism varied according to the severity of inflammation, and neither was homogeneously suppressed during the acute stage of myocarditis, but the difference decreased during the subacute stage. Our results suggest that the ratio of BMIPP uptake to that of Tl (BM/Tl) indicates the regional severity of myocarditis at each stage, and myocardial SPECT with ^{201}Tl and BMIPP could be applicable to the assessment of the severity.

Radionuclide imaging is a useful, non-invasive technique that can evaluate cardiac performance, myocardial perfusion and metabolism in ischemic and non-ischemic heart disease.¹³⁻¹⁶ Radiolabeled antimyosin antibody has been used to detect myocarditis.^{17,18} In contrast, ^{201}Tl and BMIPP were used in the current study. The myocardial distribution of ^{201}Tl depends on regional coronary flow and closely parallels regional myocardial perfusion. Since injected ^{201}Tl is considered to be transported by the Na-K ATPase system,¹⁹ ^{201}Tl myocardial uptake is considered to reflect a good general state of myocardial perfusion and unimpaired energy metabolism in myocardial cells which support Na-K ATPase.

In acute myocarditis, there is an interstitial inflammatory reaction, and it is not uncommon for fibrous tissue to be deposited and replace myocardial cells.^{20,21} Usually this process is diffuse throughout the myocardium, and inflammatory damage to myocytes might lead to dysfunc-

tion of the membrane bound Na-K ATPase system and hence to inability of myocardial cells to incorporate ^{201}Tl . Cellular damage in the myocardium after myocarditis, revealed by endomyocardial biopsy, is characterized by cellular infiltration, cell lysis, interstitial edema, fibrosis and degeneration.^{20,21} Focal myocardial damage was also reported in a significant percentage of patients with myocarditis.²² Coronary involvement is rare in myocarditis.²⁰ Coupled with our observation about the recovery of Tl uptake at the subacute stage, the inhomogeneous uptake of ^{201}Tl at the acute stage may be caused by the cellular damage induced by inflammation.

Free fatty acid is a major substrate for cardiac energy generation.^{4,23} The myocardial uptake of BMIPP has been reported to depend on the intracellular ATP level.^{24,25} The degree to which the inflammatory changes disturb aerobic energy metabolism remains unclear. Nevertheless, it is reasonable to consider that the depressed uptake of BMIPP in myocarditis is due to the inflammatory changes and parallels the severity of damage.

Our study indicated that myocardial BMIPP uptake is more sensitive to inflammatory damage than ^{201}Tl uptake. The depression of myocardial BMIPP uptake continues till the subacute stage when inflammatory cell infiltration has almost disappeared. The post-myocarditic heart has almost normal microscopic features because of the disappearance of inflammatory changes. In this condition, the depression of myocardial BMIPP uptake may be the only sign of post-inflammation. The disorder in free fatty acid metabolism, which can be estimated by BMIPP imaging, continues longer than the changes in ^{201}Tl images. The intracellular ATP level is one of the major determinants of myocardial uptake of both tracers. The difference between the two tracers may be due to the intracellular ATP compartmentation in the myocardium.²⁶⁻²⁸ ATP generation for intracellular ion handling based on glycolysis, i.e., ATP related to ^{201}Tl uptake, may be more robust than that based on aerobic metabolism, i.e., ATP for BMIPP uptake.

In our study, the regional ratio of BMIPP uptake to that of Tl (BM/Tl) showed discrepancy with that in a whole heart. We did not quantitate the area of different severity, but normalized the regional data with those for total uptake. The discrepancy may be caused by the difference between BMIPP and Tl in uptake abnormality. Our data indicate that BM/Tl is affected not only by the severity but also by the stage. It is therefore necessary to take these factors into account when interpreting the BM/Tl data.

In conclusion, our study has indicated that myocardial perfusion and aerobic metabolism were discrepant and inhomogeneously suppressed with increasing severity of inflammation in myocarditis during the acute stage of myocarditis, but that these differences recover with healing. Examination with ^{201}Tl and BMIPP and the ratio of BMIPP uptake to that of Tl may provide the information about the severity of myocarditis at each stage.

ACKNOWLEDGMENT

The authors thank Akiyoshi Yanai for technical support.

REFERENCES

1. Wenger NK. Myocarditis. In "The Heart", edited by Hurst JW, Logue RB, Schlant RC, Wenger NK. New York, McGraw-Hill; pp. 1529-1556, 1978.
2. Seko Y, Ishiyama S, Nishikawa T, Kasajima T, Hiroe M, Kagawa N, et al. Restricted usage of T cell receptor V alpha-V beta genes in infiltrating cells in the hearts of patients with acute myocarditis and dilated cardiomyopathy. *J Clin Invest* 96: 1035-1041, 1995.
3. Olinde KD, O'Connell JB. Inflammatory heart disease: pathogenesis, clinical manifestations, and treatment of myocarditis. *Annu Rev Med* 45: 481-490, 1994.
4. Bing RJ, Siegel A, Ungar J, Gilbert M. Metabolism of the human heart. *Am J Med* 16: 504-515, 1954.
5. Lochner A, Kotze JCN, Benade AJ, Gevers W. Mitochondrial oxidative phosphorylation in low-flow hypoxia: role of free fatty acids. *J Mol Cell Cardiol* 10: 857-875, 1978.
6. Weiss ES, Hoffman EJ, Phelps ME, Welch MJ, Henry PD, ter-Pogossian MM, et al. External detection and visualization of myocardial ischemia with ^{14}C -substrates *in vivo*. *Circ Res* 39: 24-32, 1976.
7. Schon HR, Schelbert HR, Robinson G, Najafi A, Huang SC, Hansen H, et al. C-11 labeled palmitic acid for noninvasive evaluation of regional myocardial fatty acid metabolism with positron-computed tomography. I. Kinetics of C-11 palmitic acid in normal myocardium. *Am Heart J* 103: 532-547, 1982.
8. Evans JR, Gunton RW, Baker RG, Beanlands DS, Spears JC. Use of radioiodinated fatty acids for photoscans of heart. *Circ Res* 16: 1-10, 1965.
9. Robinson GD, Lee AW. Radioiodinated fatty acids for heart imaging: Iodine monochloride addition compared with iodine replacement labeling. *J Nucl Med* 16: 17-21, 1975.
10. Goodman MM, Kirsch G, Knapp FF Jr. Synthesis and evaluation of radioiodinated terminal p-iodophenyl-substituted- and β -methyl-branched fatty acids. *J Med Chem* 27: 390-397, 1984.
11. Nishimura T, Uehara T, Shimonagata T, Nagata S, Haze K. Clinical results with β -methyl-p-(^{123}I)iodophenylpentadecanoic acid, single-photon emission computed tomography in cardiac disease. *J Nucl Cardiol* 1: S65-S71, 1994.
12. Kodama M, Hanawa H, Saeki M, Hosono H, Inomata T, Suzuki K, et al. Rat dilated cardiomyopathy after autoimmune giant cell myocarditis. *Circ Res* 75: 278-284, 1994.
13. Tamaki N, Tadamura E, Kudo T, Hattori N, Inubushi M, Konishi J. Recent advances in nuclear cardiology in the study of coronary artery disease. *Ann Nucl Med* 11: 55-66, 1997.
14. Franken PR, Dendale P, Block P. Clinical nuclear cardiology: flow tracers and free fatty acid analogs to detect viable myocardium after infarction. *Acta Cardiol* 51: 501-514, 1996.
15. Nishimura T. Current status of nuclear cardiology in Japan. *J Nucl Cardiol* 3: 422-427, 1996.
16. Tamaki T, Fujibayashi Y, Nagata Y, Yonekura Y, Konishi

- J. Radionuclide assessment of myocardial fatty acid metabolism by PET and SPECT. *J Nucl Cardiol* 2: 256–266, 1995.
17. Matsumori A, Ohkusa T, Matoba Y, Okada I, Yamada T, Kawai C, et al. Myocardial uptake of antimyosin monoclonal antibody in a murine model of viral myocarditis. *Circulation* 79: 400–405, 1989.
 18. Narula J, Khaw BA, Dec GW, Palacios IF, Newell JB, Southern JF, et al. Diagnostic accuracy of antimyosin scintigraphy in suspected myocarditis. *J Nucl Cardiol* 3: 371–381, 1996.
 19. Weich HF, Strauss HW, Pitt B. The extraction of Thallium-201 by the myocardium. *Circulation* 56: 188, 1977.
 20. Fenoglio JJ Jr, Ursell PC, Kellogg CF, Drusin RE, Weiss MB. Diagnosis and classification of myocarditis by endomyocardial biopsy. *N Engl J Med* 308: 12–18, 1983.
 21. Aretz HT. Myocarditis: the Dallas criteria. *Hum Pathol* 18: 619–624, 1987.
 22. Lieberman EB, Hutchins GM, Herskowitz A, Rose NR, Baughman KL. Clinicopathologic description of myocarditis. *J Am Coll Cardiol* 18: 1617–1626, 1991.
 23. Ballard FB, Donforth WH, Naegel S, Bing RJ. Myocardial metabolism of fatty acids. *J Clin Invest* 39: 717–723, 1960.
 24. Fujibayashi Y, Yonekura Y, Takemura Y, Wada K, Matsumoto K, Tamaki N, et al. Myocardial accumulation of iodinated beta-methyl-branched fatty acid analogue, iodine-125-15-(p-iodophenyl)-3-(R,S)methylpentadecanoic acid (BMIPP), in relation to ATP concentration. *J Nucl Med* 31: 1818–1822, 1990.
 25. Yamamichi Y, Kusuoka H, Morishita K, Shirakami Y, Kurami M, Okano K, et al. Metabolism of iodine-123-BMIPP in perfused rat hearts. *J Nucl Med* 36: 1043–1050, 1995.
 26. Campbell JD, Paul RJ. The nature of fuel provision for the Na⁺, K⁺-ATPase in porcine vascular smooth muscle. *J Physiol* 447: 67–82, 1992.
 27. Weiss JN, Lamp ST. Glycolysis preferentially inhibits ATP-sensitive K⁺ channels in isolated guinea pig cardiac myocytes. *Science* 238: 67–69, 1987.
 28. Kusuoka H, Marban E. Mechanism of the diastolic dysfunction induced by glycolytic inhibition. *J Clin Invest* 93: 1216–1223, 1994.